Functional Interactions in Bacteriorhodopsin: A Theoretical Analysis of Retinal Hydrogen Bonding with Water

Mafalda Nina,* Benoît Roux,‡ and Jeremy C. Smith*

*Section de Biophysique des Protéines et des Membranes, Département de Biologie Cellulaire et Moléculaire, C.E.A., Centre d'Etudes Saclay, 91191 Gif-sur-Yvette Cedex, France, and ‡Groupe de Recherche en Transport Membranaire (GRTM), Department of Chemistry, University of Montreal, C.P. 6128, succ. A, Montreal, Quebec, Canada H3C 3J7

ABSTRACT The light-driven proton pump, bacteriorhodopsin (bR) contains a retinal molecule with a Schiff base moiety that can participate in hydrogen-bonding interactions in an internal, water-containing channel. Here we combine quantum chemistry and molecular mechanics techniques to determine the geometries and energetics of retinal Schiff base-water interactions. Ab initio molecular orbital calculations are used to determine potential surfaces for water-Schiff base hydrogen-bonding and to characterize the energetics of rotation of the C—C single bond distal and adjacent to the Schiff base NH group. The ab initio results are combined with semiempirical quantum chemistry calculations to produce a data set used for the parameterization of a molecular mechanics energy function for retinal. Using the molecular mechanics force field the hydrated retinal and associated bR protein environment are energy-minimized and the resulting geometries examined. Two distinct sites are found in which water molecules can have hydrogen-bonding interactions with the Schiff base: one near the NH group of the Schiff base in a polar region directed towards the extracellular side, and the other near a retinal CH group in a relatively nonpolar region, directed towards the cytoplasmic side.

INTRODUCTION

Bacteriorhodopsin (bR) is a membrane protein that functions as a light-driven proton pump in the purple membrane of the bacterium *Halobacterium halobium* (Oesterhelt and Stoeckenius, 1971). The light-absorbing chromophore is a retinal molecule that is covalently bonded via its Schiff base to the ϵ-amino group of Lys-216 (Rothschild et al., 1982). The characteristic purple color of bacteriorhodopsin is due to absorption by the chromophore. The absorption is red-shifted with respect to that of related model compounds in solution, an effect that has been proposed to originate from interactions between the retinal and its environment in the protein (Mathies et al., 1991).

The retinal interactions may include hydrogen bonds with the protonated Schiff base. Although the direct identification of Schiff base hydrogen bonds using diffraction techniques has not yet been possible, a structure for bR at relatively high resolution has been obtained (Henderson et al., 1990). This revealed a channel through the protein that includes the Schiff base. Site-directed mutagenesis experiments suggest that the channel contains the pathway for proton transfer through bR (Mogi et al., 1987; Mogi et al., 1988; Stern and Khorana, 1989; Marti et al., 1991). Low resolution neutron diffraction using contrast variation has indicated that about four water molecules are present in the neighborhood of the Schiff base, although their positions in the direction perpendicular to the membrane plane could not be accurately determined (Papadopoulos et al., 1990). There is, however, considerable evidence that water molecules are directly associated with the Schiff base. A resonance Raman study suggests that a negatively charged counterion located near the Schiff base group is stabilized by water molecules (Hildebrandt and Stockburger, 1984). Solid state ^{13}C and ^{15}N NMR experiments led to a model being proposed in which a water molecule is directly hydrogen-bonded to the Schiff base (De Groot et al., 1990). Other solid state ^{1}H and ^{15}N NMR experiments suggest that there is a direct exchange of the Schiff base NH hydrogen with bulk water (Harbison et al., 1988). A very recent resonance Raman study of the Schiff base hydrogen/deuterium exchange also led to the conclusion that a water molecule is directly hydrogen-bonded to the Schiff base NH proton (Deng et al., 1994).

A detailed understanding of Schiff base hydrogen-bonding in the various stages of the photocycle will be required for a complete description of bR function. That hydrogen-bonding significantly perturbs the electronic structure of retinal has been inferred from spectroscopic work (Hildebrandt and Stockburger, 1984). Moreover, the Schiff base participates directly in the proton transfer, which is probably mediated by hydrogen-bonding interactions (Zundel, 1986; Cao et al., 1991; Rothschild et al., 1992; Rath et al., 1993). Recent work using synthetic retinal protonated Schiff bases lends further support to the idea that Schiff base hydration may play an important functional role (Gat and Sheves, 1993). The retinal protonated Schiff bases were synthesized with

Received for publication 22 June 1994 and in final form 12 October 1994.

Address reprint requests to Dr. Jeremy C. Smith, Section de Biophysique des Protéines et des Membranes, Department de Biologie Cellulaire et Moléculaire, C.E.A. Centre d'Etudes Saclay, 91191 Gif-sur-Yvette, Cedex, France. Tel.: 33-1-69086717; Fax: 33-1-69088139; E-mail: jeremy@tobit.saclay.cea.fr.

Abbreviations used: bR, bacteriorhodopsin; NMR, nuclear magnetic resonance; CPU, computer processor unit; NMP, (*E'*)-*N*-methyl-2-propylidenimine (*s-trans*); RMS, root mean square; AM1, Austin method 1; NPR, *N*-propyl retinylidenimine (all *trans*); CHARMM, Chemistry at HARvard Macromolecular Mechanics; RHF, Restricted Hartree-Fock; NMB, (*E'*)-*N*-methyl-2-*cis*-butenylidenimine; MP2, Møller-Plesset Second-Order Perturbation.

0006-3495/95/01/25/15 $2.00

incorporated carboxyl groups. The pK_a of the synthesized Schiff base was found to be sensitive to the orientation of the carboxyl group with respect to the NH bond. The results were interpreted in terms of the presence of one or more water molecules bridging the two groups in the high pK_a compound and stabilizing the protonated form relative to the unprotonated form.

A direct determination of the hydrogen-bonding arrangement will require additional experimental work. However, computational chemistry has an important role to play in identifying and quantifying hydrogen-bonding geometries and energies of pertinent model systems. Ab initio quantum chemical calculations, when performed with a large enough basis set, give reliable estimates of geometries and interaction energies in hydrogen-bonded complexes (Hehre et al., 1986). Because ab initio calculations are computationally intensive, the CPU time required increasing with approximately the fourth power of the number of atomic orbitals in the system, applications are presently restricted to fragments of retinal. Previous ab initio calculations indicated that water molecules can form two stable hydrogen-bonded complexes with a model Schiff base, (*E*)-*N*-methyl-2-propenylidenimine (*s-trans*) $[CH_2{=}CH{-}CH{=}NH{-}(CH_3)]^+$, which we call here NMP (Nina et al., 1993). In one complex, hereafter referred to as complex A, the water molecule hydrogen-bonds to the NH group of the Schiff base. In bR before photon absorption, the NH group is oriented towards the extracellular side of the membrane. In the second complex, hereafter referred to as complex B, the water hydrogen-bonds to a retinal CH group, on the opposite side of the molecule, oriented towards the cytoplasmic side of the membrane. Ab initio calculations of vibrational spectra of a similar model Schiff base have been recently reported (Deng et al., 1994).

In the present paper, calculations using ab initio and semiempirical quantum chemical methods and molecular mechanics are used to analyse ground-state retinal Schiff base hydrogen-bonding properties and associated conformational energetics. The ab initio calculations are used to obtain potential surfaces for water-Schiff base hydrogen-bonding interactions and a potential energy curve for the rotation around the N=C—C=C single bond. The model compounds and their nomenclature used are illustrated in Fig. 1. Most of the ab initio calculations are performed with the model compound NMP. The charge distribution on retinal and retinal-water interactions are investigated with semiempirical quantum chemical calculations using the AM1 method (Dewar et al., 1985) using a model of the whole retinal protonated Schiff base, *N*-propyl retinylidenimine (all-*trans*)-$[CH_3\text{-}CH_2\text{-}CH_2\text{-}NH{=}C15\text{-}C14{=}C13(CH_3)\text{-}C12{=}C11\text{-}C10{=}C9(CH_3)\text{-}C8{=}C7\text{-}C6\cdots]^+$, which we call here NPR. As quantum chemistry calculations on retinal including the protein are presently impractical, questions about the structural and energetic properties of water molecules hydrogen-bonded to the Schiff base in bR must be addressed using an appropriately parameterized molecular mechanics potential energy function. Therefore, we use the information obtained from the quantum chemical calculations to parameterize the CHARMM molecular mechanics energy function (Brooks et al., 1983). Using the molecular mechanics function energy minimizations are performed of the retinal together with its protein environment and one and two water molecules. Resulting interactions of the water molecules with retinal and bR are described.

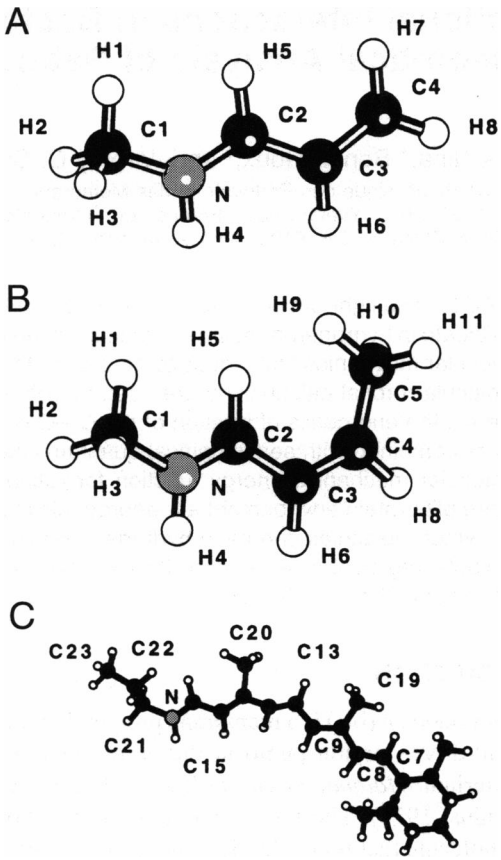

FIGURE 1 Models for the protonated retinal Schiff bases: (*A*) (*E*)-*N*-methyl-2-propenylidenimine (NMP), (*B*) (*E*)-*N*-methyl-2-butenylidenimine (NMB); and (*C*) *N*-propyl retinylidenimine (NPR). The atom shadings are as follows: white = hydrogen, black = carbon, gray = nitrogen.

In Materials and Methods, the methods used for performing the quantum chemical calculations are described and the strategy adopted for parameterizing the molecular mechanics energy function is detailed. In Results and Discussion, the characteristics of the ab initio Schiff base-water complexes are described together with the interaction energy as function of the hydrogen-bonding distances and angles. The potential energy as a function of rotation around the C—C single bond distal to the Schiff base nitrogen is calculated and compared with that of related compounds. Corresponding interaction energy and rotational potential curves calculated using the parameterized molecular mechanics energy function are given and decomposed. Semiempirical quantum chemistry calculations on NPR are performed and its charge distribution and interactions with water are discussed. Finally, energy minimizations of bR incorporating the new force field information are described. The calculations provide a basis

for the quantitative description of functionally important hydration interactions in bR.

MATERIALS AND METHODS

Ab initio calculations

Ab initio calculations were performed using the GAUSSIAN 90 program (Frisch et al., 1990) on a Silicon Graphics SGI/480 Power Series computer. The calculations were performed at the Restricted Hartree-Fock (RHF) level with a 6–31G* basis set. Calculations on cationic complexes have been shown to give reliable results at this level (Zheng and Merz, 1992; Koller and Hadži, 1993). This was confirmed in our previous investigation, in which geometry optimizations and interaction energy calculations were performed for NMP-water complexes using basis sets larger than 6–31G* and including electron correlation corrections (Nina et al., 1993). It was found that at the higher levels of theory the intra- and intermolecular geometries varied only slightly and the interaction energies remained within ~10% of the RHF/6–31G* values.

In the present work, RHF/6–31G* calculations were performed for the dependence of the interaction energies on radial and angular variables describing the hydrogen-bonding geometries. We define the interaction energy of a complex as the difference between the energy of the complex and the sum of the energies of the isolated nonoptimized components, i.e., with their internal geometries fixed at those of the complex. To reduce the computational workload, the intramolecular geometry of the cation was fixed at that of the energy minimum-optimized isolated molecule such that the complex preserves overall C_s geometry with a methyl C—H bond staggered with respect to the N=C2 bond. In the molecular mechanics calculations the TIP3P model (Jorgensen et al., 1983), modified as currently in use in CHARMM, was used for the water molecules. In the ab initio calculations, the water molecule was constrained to the experimental geometry for consistency with the TIP3P water model (Jorgensen et al., 1983). The plane of the water molecule was kept orthogonal to the protonated Schiff base symmetry plane, as in the minimum energy hydrogen-bonding arrangement (Nina et al., 1993). Subject to the above constraints, the RHF/6–31G* interaction energy was calculated as a function of r_{OH}, the distance between the hydrogen-bonding hydrogen and the water oxygen and θ, the angle between the X-H axis of the Schiff base (N—H4 for complex A and C2—H5 for complex B) and the symmetry axis of the H_2O. r_{OH} and θ are illustrated in Fig. 2.

An optimization of the complex of NMP with two water molecules was performed; this leads to only minor changes in the hydrogen-bonding properties that are not discussed. An additional set of ab initio calculations was performed on (*E*)-*N*-methyl-2-*cis* butenylidenimine, CH3—NH=CH—CH=CH(CH3)$^+$, which we call here NMB, to examine the influence of the C5 methyl group (corresponding to the C20 methyl group bound to C13 in retinal) on the water-Schiff base intermolecular geometry and interaction energy. Again, only small differences were seen in the geometries and interaction energies obtained.

The ab initio C2-C3 rotational potential energy curve for the isolated NMP molecule was calculated starting from the optimized NMP geometry. Geometry optimization was performed at each rotational point with all the X-C2-C3-Y dihedrals constrained, where X=N,H5 and Y=C4,H6.

Semiempirical calculations

Semiempirical quantum chemical calculations were carried out with AM1 (Dewar et al., 1985) as implemented in the MOPAC program, on an IBM RISC 6000 workstation. AM1 geometry optimizations were carried out on the isolated components (NMP, NPR, water) and on complexes A and B of NMP and NPR with water. For NMP the ab initio optimized geometries were used as starting geometries for the AM1 optimizations, and the dihedral angles were constrained at the ab initio values. The NMP-water complexes were constrained to C_s symmetry. The starting geometry for the NPR optimization was taken from a high resolution x-ray analysis of 6-*s*-*cis* retinal (Hamanaka et al., 1972) with the C5=C6—C7=C8 dihedral angle rotated to 180° to produce all-*trans* retinal. The starting coordinates of the N16, C15, C14, C13, C20, and associated hydrogen atoms were taken from the ab initio optimized geometry of NMB and those of the propyl group bound to the nitrogen (C23—C22—C21—) were taken from the experimental bR coordinates for the Lys-216 side chain (Henderson et al., 1990). As in the ab initio calculations, the internal water geometry was constrained to that of TIP3P. Starting values for the intermolecular geometries for the NPR-water complexes A and B were those obtained from the ab initio calculations on NMB-water complexes.

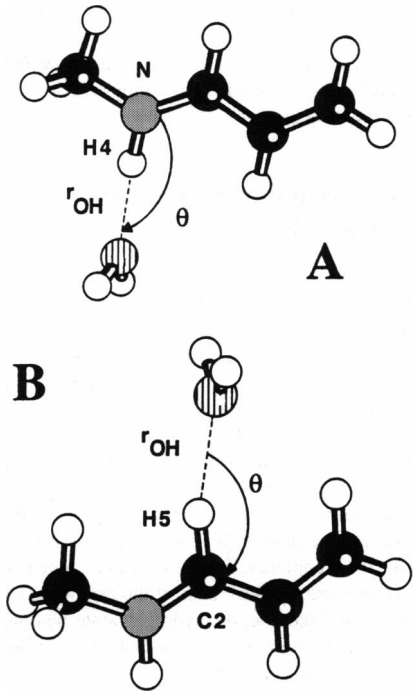

FIGURE 2 Ab initio optimized geometries for NMP-water complexes A and B.

Molecular mechanics force field

The molecular mechanics program used is CHARMM (Brooks et al., 1983). The form of the potential energy, V, is

$$V = \sum_{\text{bonds}} k_b(b - b_0)^2 + \sum_{\text{angles}} k_\theta(\theta - \theta_0)^2 + \sum_{\text{dihedrals}} \sum_{n=1}^{N} k_\phi^{(n)}[1 + \cos(n\phi - \delta_n)] + \sum_{\text{impropers}} k_\omega(\omega - \omega_0)^2 + \sum_{i,j} 4\epsilon_{ij}\left[\left(\frac{\sigma_{ij}}{r_{ij}}\right)^{12} - \left(\frac{\sigma_{ij}}{r_{ij}}\right)^{6}\right] + \sum_{i,j}\left(\frac{q_i q_j}{Dr_{ij}}\right) e_{14}(i,j) \quad (1)$$

In Eq. 1 b, θ, and ω are the bond lengths, valence angles, and improper dihedrals, respectively, for which b_0, θ_0, and ω_0 are the reference values, and k_b, k_θ, and k_ω are the force constants. The dihedral torsion potential is a sum of cosine functions in a Fourier series expansion, where ϕ is the dihedral angle, δ_n is the phase angle, and $k_\phi^{(n)}$ is the force constant of the nth term. The nonbonded interactions, for atom pairs i and j separated by distance r_{ij} consist of a 12–6 Lennard-Jones van der Waals term with potential well-depth ϵ_{ij}. Van der Waals interactions for atom pairs are calculated according to the mixing rules: $\sigma_{ij} = 1/2(\sigma_{ii} + \sigma_{jj})$ and $\epsilon_{ij} = \sqrt{\epsilon_{ii}\epsilon_{jj}}$. The minimum energy distance is $r_{min} = 2^{1/6}\sigma_{ij}$. The Coulombic term represents interactions between atomic partial charges, q_i, q_j. The relative dielectric constant, D, is taken as 1. The $e_{14}(i,j)$ factor corresponding to the scaling of the van der Waals and electrostatic interactions involving atoms separated by three

bonds was taken as 1. There is no explicit hydrogen-bonding term in the potential energy function; hydrogen bonds are represented by the electrostatic and van der Waals terms. For the energy minimizations of bR, the electrostatic interactions were smoothed by multiplication by a cubic switching function between 10 and 12 Å.

Derivation of molecular mechanics force field parameters

The molecular mechanics parameter set derived by fitting to the quantum mechanical calculations is given in the Appendix. The parameters were obtained by manual adjustment of a set taken from chemically similar atom types in the CHARMM (Version 22) force field. An initial adjustment of the bond and angle parameters was made to obtain an energy-minimized structure for NMP in agreement with the ab initio optimized geometry. The parameter set obtained from the calculations on the isolated Schiff base was refined using molecular mechanics energy minimizations of the NMP—water complexes A and B. This involved the adjustment of nonbonded parameters (Lennard-Jones and electrostatic) to reproduce the ab initio interaction energies and intermolecular geometries at the energy minimum configurations for the complexes. Lennard-Jones parameters for the atom types CTR and HAR were taken as those of the existing CT and HA atom types in the force field. Likewise, the hydrogen atom binding the nitrogen (HCR*) was given the HC atom type and the carbon (sp^2) (CR*) the C atom type (* refers to a wild-card character). For the other atom types (NCH* planar (sp^2) nitrogen, HPL* and HPM* polar hydrogens), the van der Waals radius (r_{min}) was modified, keeping $\epsilon_{i,i}$ unchanged. The TIP3P parameterization of the water molecules was unchanged. All minimizations of complexes were performed to RMS energy gradients <2 10^{-4} kcal/mol/Å.

A final parameterization involved the torsional terms for the NMP N=C2—C3=C4 rotational potential curve. The molecular mechanics rotational potential was obtained as for the ab initio curve by constraining the required dihedrals and minimizing the potential energy due to the other terms, i.e., adiabatically. At all points on the rotational potential curve, the RMS energy gradient obtained was <10^{-4} kcal/mol/Å except for the maximum-energy conformation at 100°, where the RMS energy gradient was ~6.10^{-4} kcal/mol/Å.

The final NMP parameter set was subjected to a test by calculating the complex A and B interaction energies with water as a function of the intermolecular variables (r_{OH} and θ) defined in Ab Initio Calculations. In the calculation of the intermolecular interaction energies, the same procedure was followed as for the ab initio calculations, i.e., the internal geometries of both molecules of each complex were fixed at the optimized energy-minimum ab initio values.

The energy function for NMP was used as a basis for the development of an energy function for the retinal protonated Schiff base, NPR. The bond length and angle reference values (b_0 and θ_0) and force constants (k_b and k_θ) for the Schiff base moiety [· · ·N16H16=C15H15—C14H14=C13· · ·]$^+$ were transferred from the NMP ab initio optimized geometry. All other force constants were taken from similar bonds and angles of the CHARMM 22 force field. The NMB ab initio calculations were used to obtain an optimized geometry for the C20 methyl group binding the C13 atom. b_0 and θ_0 values for [· · ·C13—C12H12=C11H11—C10H10=C9—C19—C8H8=C7H7—C6· · ·] were set at the x-ray geometry of 6-*s*-*cis* retinal (Hamanaka et al., 1972). The C2—C3 torsional terms for NMP were transferred to the C15—C14 dihedral in NPR. The remaining C—C single-bond dihedral force constants (k_ϕ), i.e., C13—C12, C11—C10, C9—C8, and C7—C6 were transferred from the C—C rotational potential derived for butadiene (Nina et al., 1992). The k_ϕ values for the polyene chain double bonds were taken from a valence bond calculation on decapentene (Said et al., 1984).

Molecular mechanics energy minimization of bR

Two energy minimizations were performed on bR: one with the one water molecule of complex A and one with the two water molecules of complexes A and B. The published bR structure (Henderson et al., 1990) was modified by ~4 Å shift of helix D towards the cytoplasmic side of the membrane (Henderson, personal communication). In the dark, bacteriorhodopsin exists in an equilibrium between two forms, bR_{568} and bR_{555}, the subscripts referring to absorption maxima. In bR_{568} the retinal moiety is in the all-*trans* configuration, whereas in bR_{555} it is 13-*cis* (Oesterhelt and Stoeckenius, 1973; Sperling et al., 1977; Pettei et al., 1977). On extended exposure to light, bR_{555} is converted to bR_{568}. In the present calculations, the retinal was taken in the all-*trans* conformation as in the bR_{568} form (Harbison et al., 1984a, b; Smith et al., 1989).

For the minimizations on both complexes, a two-stage protocol was adopted. In both stages, certain atoms were fixed and others allowed to move, and a series of three 300-step ABNR minimizations were performed. During the three minimizations, harmonic restraints were placed on the atoms allowed to move with force constants of 10, 5, 1, and 0 kcal/mol/Å^2, respectively.

Stage (i) The positions of the water molecule, N16, H16, C15, H15, and all atoms further than 10 Å from any retinal atom were fixed.

Stage (ii) The water molecule, the retinal, and all atoms within 10 Å of any retinal atom were then allowed to move. Atoms further than 10 Å from any retinal atom were then allowed to move. The other atoms were fixed.

The final RMS energy gradient was 0.018 kcal/mol/Å for the minimization of bR with one water molecule and 0.092 kcal/mol/Å with two water molecules.

RESULTS AND DISCUSSION

The energy function developed here has been parameterized to reproduce the energy changes as a function of the soft degrees of freedom of the retinal and its complexes with water. This requires an accurate representation of the torsional barriers and the nonbonded interactions involving van der Waals and electrostatic effects. The resulting energy function can be used to probe the flexibility of protonated retinal and its possible hydrogen-bonding associations in bR.

The protonated Schiff base, NMP

The minimum energy geometries for the isolated, geometry-optimized NMP molecule obtained from the ab initio, semiempirical, and molecular mechanics calculations are listed in Table 1. The RMS coordinate deviation between the molecular mechanics and ab initio geometries is 0.052 Å. The bond lengths agree to within 0.02 Å and the bond angles to within 2°.

Most of the flexibility of the Lys-216-retinal segment arises from torsions around single bonds. The ab initio potential for rotation around the C2—C3 bond of NMP is shown in Fig. 3 *A*. Two minima exist; the lowest energy conformer is *trans*, and the other minimum is a *gauche* configuration at ~25°. The height of the *trans-gauche* barrier is ~9.9 kcal/mol with the maximum at ~100°. The potential is quite flat at the *gauche* conformation, a 10° change in the torsional angle being accompanied by only a 0.03 kcal/mol energy difference. The energy difference between the *cis* and *gauche* conformations is ~0.2 kcal/mol.

Significant bond length changes were observed in the ab initio calculation when optimizing the geometry at each rotational step. The C2—C3 single bond length increases by ~0.04 Å going from the *trans* form to 90° and then decreases by ~0.03 Å at the *cis* form. The C3=C4 bond length decreases by ~0.01 Å going from 180° to 90° then increases by the same amount going to the cis conformation. These

TABLE 1 Ab initio, semiempirical, and molecular mechanical (MM) optimized geometries for isolated NMP and NMP-water complexes A and B

	Ab initio			AM1			MM
	NMP	A	B	NMP	A	B	NMP
Bond lengths (Å)							
C4═C3	1.331	1.329	1.331	1.345	1.343	1.345	1.337
C2—C3	1.440	1.445	1.441	1.446	1.449	1.447	1.447
H7—C4	1.076	1.076	1.075	1.102	1.102	1.106	1.080
H8—C4	1.074	1.074	1.074	1.104	1.103	1.103	1.081
H6—C3	1.075	1.074	1.075	1.106	1.110	1.105	1.076
N═C2	1.278	1.274	1.280	1.314	1.313	1.315	1.285
H5—C2	1.076	1.077	1.078	1.118	1.117	1.124	1.085
H4—N	1.003	1.014	1.003	1.009	1.016	1.008	1.023
C1—N	1.469	1.465	1.467	1.446	1.445	1.446	1.491
H1—C1	1.079	1.080	1.079	1.123	1.125	1.124	1.087
H2—C1	1.080	1.080	1.080	1.126	1.123	1.125	1.087
H3—C1	1.080	1.080	1.080	1.126	1.123	1.125	1.087
Bond Angles (deg)							
C2—C3═C4	119.7	119.7	118.8	121.2	121.3	120.2	121.0
H7—C4═C3	122.3	122.3	121.6	123.5	123.5	122.6	122.1
H6—C3═C4	121.7	121.2	122.0	120.5	121.2	121.1	123.0
N═C2—C3	124.2	123.7	123.9	124.1	123.5	124.1	122.6
H4—N═C2	117.9	118.0	118.4	120.2	120.1	120.3	116.1
H1—C1—N	109.3	109.5	108.9	111.1	111.2	111.1	111.0
H2—C1—N	109.0	109.1	109.2	109.0	108.9	109.0	109.6
H3—C1—N	109.0	109.1	109.2	109.0	108.9	109.0	109.6
Water							
d_{H-O}		0.950			0.963		
Θ_{H-O-H}		106.0			106.3		
Intermolecular Distances and Angles							
$d_{H4\cdots O}$		1.870			2.044		
$\Theta_{N-H4\cdots O}$		175.5			152.5		
Water							
d_{H-O}			0.950			0.963	
Θ_{H-O-H}			105.5			104.5	
Intermolecular Distances and Angles							
$d_{H5\cdots O}$			2.103			2.115	
$\Theta_{C2-H5\cdots O}$			168.8			151.3	

results are consistent with a reduction in conjugation on deviation from the planar configurations.

The fitted molecular mechanics NMP rotational potential and a decomposition of the contributing terms are presented in Fig. 3 *A*. The form of the ab initio C2—C3 rotational curve is closely reproduced by the molecular mechanics potential. The molecular mechanics potential curve was obtained including the first four sinusoidal terms in the Fourier series for the intrinsic dihedral contribution; the parameters for these are given in the Appendix. The inclusion of higher-order terms was also found to be necessary in calculations on butadiene (Nina et al., 1992). This is in contrast with simpler systems, such as *n*-butane, for which low symmetry rotational potentials can sometimes be conveniently modelled using a combination of a single torsional term and nonbonded interactions (Smith and Karplus, 1992). The shape of the NMP molecular mechanics potential curve in Fig. 3 *A* is significantly influenced by the torsional, bond angle, and nonbonded terms in the *cis* and *gauche* conformations.

A common procedure in molecular mechanics force fields is to scale the 1,4 electrostatic interaction energy, i.e., between atoms separated by three bonds. As has been documented in studies on alkanes, this can qualitatively change conformational energy differences (Smith and Karplus, 1992). In the present case, it was found that when the 1,4 electrostatic interactions are multiplied by a scaling factor of 0.5 the electrostatic energy stabilizes the *cis* conformer by 1.82 kcal/mol relative to the *trans* conformer. The *gauche* conformer vanishes, and the *cis* configuration becomes a minimum on large, flat potential well. It is therefore essential to not scale the 1,4 electrostatic interactions in calculations using the force field developed here.

Previous ab initio calculations, on the unprotonated NMP Schiff base, at the same level of theory gave a value for the *trans-gauche* barrier of ~7.5 kcal/mol (Kontoyianni et al., 1992), i.e., smaller than that of the protonated form by ~1.5 kcal/mol. Therefore, protonation of the Schiff base increases the barrier to rotation around the C2—C3 single bond. This is consistent with the ab initio result that the C2—C3 bond length for the *trans* unprotonated Schiff base is 0.03 Å longer than in the *trans* protonated molecule (Nina et al., 1993).

In Fig. 3 *B* the C2—C3 rotational potential is compared with the relatively well characterized C2—C3 rotation in 1,3-butadiene (CH_2═CH—CH═CH_2) (Guo and Karplus, 1991; Nina et al., 1992). Differences between protonated NMP and butadiene are expected to be due mainly to the

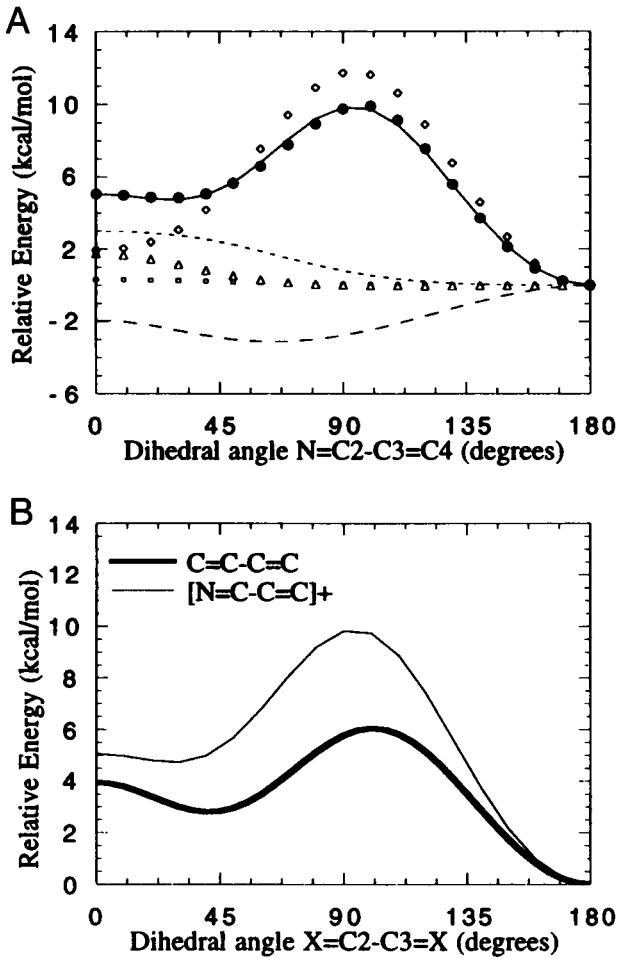

FIGURE 3 (*A*) Ab initio and molecular mechanical C2—C3 rotational potential energy curves for NMP. The components of the molecular mechanics potential energy are also plotted. (●) RHF/6-31G*, (——) molecular mechanics, (- - - -) VDW, (– – –) elec, (◇) dihedrals, (□) bonds, (△) angles. The *cis* conformation is at 0°, and the *trans* conformation is at 180°. (*B*) Molecular mechanical C2—C3 rotational potential energy curves for NMP and butadiene. Both curves were determined by fitting to ab initio results.

presence in NMP of the positive charge and the nitrogen atom instead of carbon. The *trans-gauche* barrier in butadiene is 6.4 kcal/mol, considerably smaller than that of NMP. This result suggests that the NMP C2—C3 bond has somewhat more double-bond character than the corresponding single bond in butadiene. This is consistent with the difference in length of the bonds; the C2—C3 single bond in *trans* butadiene is 0.025 Å longer than that in NMP. The *gauche* minimum is much more pronounced in butadiene than in NMP, the *cis-gauche* energy barrier being 1.1 kcal/mol in butadiene.

Schiff base-water hydrogen-bonded complexes

The interaction of a water molecule with NMP shows two energy minima on opposite sides of the molecule. The interaction energies and hydrogen-bonding geometries of the two complexes, A and B (see Fig. 2), obtained by ab initio and molecular mechanics calculations are listed in Table 2. In complex A the water oxygen hydrogen-bonds with the NH hydrogen of the Schiff base. The ab initio interaction energy for this complex is −16.5 kcal/mol. This is a relatively strong hydrogen bond; in comparison, the calculated ab initio interaction energy of the water dimer is −5.62 kcal/mol at the same level of theory (Frisch et al., 1986). In complex B the water molecule hydrogen-bonds to the C2—H5 group on the opposite side of the Schiff base. This hydrogen bond, although being of the relatively uncommon C—H· · ·O type, also has a strong interaction energy of −12.6 kcal/mol. It is somewhat less linear than in complex A.

TABLE 2 Ab initio and molecular mechanics (MM) intermolecular geometries and interaction energies for minimum-energy NMP-water complexes A and B

		Ab initio	MM
A	r_{OH} (Å)	1.87	1.83
	θ (deg)	175	177
	E_{int} (kcal/mol)	−16.5	−16.4
B	r_{OH} (Å)	2.16	2.10
	θ (deg)	159	157
	E_{int} (kcal/mol)	−12.6	−12.7

Nonbonded terms in the molecular mechanics energy function were adjusted to reproduce the ab initio energies and configurations in Table 2. The partial charges were derived starting from a Mulliken population analysis of the ab initio wavefunction of the isolated cation (Mulliken, 1955). As expected, a straight transfer of the Mulliken charges to the molecular mechanics force field does not reproduce the hydrogen-bonding interaction energies. The Mulliken charges were adjusted by defining the following groups: the methyl group, N—H4, C2—H5, C3—H6, and C4—H7H8. The net charges on each of these groups was maintained at the Mulliken values. Within each group, the charges were optimized to fit the interaction energies; this amounts to adjusting the group dipole moments. The water charges were fixed at the TIP3P values (Jorgensen et al., 1983).

The resulting molecular mechanics minimum energy distances and energies are in good agreement with the ab initio results (Table 2). A decomposition of the molecular mechanics interaction energies indicates that the principal contributions are from the electrostatic terms and are −18.46 kcal/mol for complex A and −13.30 kcal/mol for complex B. Consequently, the molecular mechanics interaction energies are sensitive to small changes in the partial charges. For example, an increase of 0.01 units of electron charge of the partial charge of H4 (decreasing the nitrogen charge by 0.01 units of electron charge to maintain the global charge) decreases the complex A interaction energy by 0.3 kcal/mol. The van der Waals interactions between the water molecules and the NMP are repulsive at the energy minima, being 2.09 kcal/mol and 0.58 kcal/mol for complexes A and B, respectively.

The ab initio radial and angular interaction energy curves for the NMP-water complexes are presented in Figs. 4, *A* and

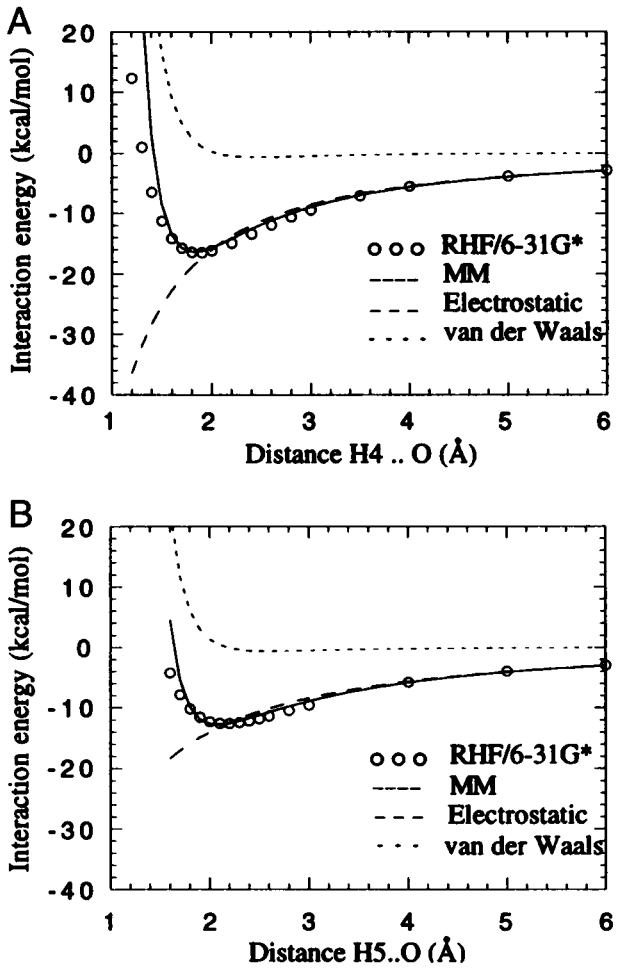

FIGURE 4 Radial dependence of the interaction energy of NMP-water complexes A and B obtained from ab initio and molecular mechanics calculations. Components of the molecular mechanical interaction energy are also plotted. (*A*) complex A with the N—H4· · ·O angle at 180°. (*B*) complex B with the C2—H5· · ·O angle at 160°.

B and 5 *A–D* together with the corresponding molecular mechanics energies and their van der Waals and electrostatic components. Complete molecular mechanical (r_{OH}, θ) potential surfaces for complexes A and B are shown in Fig. 6, *A* and *B*. Because only the minimum energy configuration for each complex was used in the parameterization of the energy function, the comparison with the ab initio results at the other points on the (r_{OH}, θ) surface constitutes an independent *test* of the accuracy of the molecular mechanical potential function. The empirical force field gives potential curves that reproduce reasonably well the ab initio results. In the radial curves (Fig. 4, *A* and *B*), significant disagreement (>0.1 kcal/mol) is observed only at energies larger than those frequently sampled during thermal fluctuations at physiological temperatures. The repulsive interaction at short distances is somewhat too steep and could probably be more accurately modelled by a $1/r^{10}$ or $1/r^{9}$ term instead of $1/r^{12}$. This difference has been observed in work on other biomolecular complexes (Lifson et al., 1979; Burkert and Allinger, 1982; Roux and Karplus, submitted for publication). However, as it affects primarily high energy configurations a modification of the functional form would not be expected to result in a significant change in the system's behavior.

Polarization effects, incompletely treated in the potential energy function, are probably responsible for the small differences in the ab initio and molecular mechanics curves at ~2.2 Å < r_{OH} < ~3.5 Å. To reproduce accurately both the position and depth of the ab initio energy minimum, it is necessary to include polarization effects implicitly by slightly overestimating the magnitude of the van der Waals attraction ($1/r^6$) in the potential function. At longer distances, the ab initio energy surface differs from the potential function because the induced polarization effects result in an attractive energy contribution that varies as $1/r^4$ to lowest order, less steeply than the radial dependence of the overestimated van der Waals attraction (Roux and Karplus, 1995, in press).

The dependence of the interaction energies on the X—H· · ·O acceptor angle for two different H· · ·O distances is presented in Fig. 5 *A–D*. As is common for hydrogen-bonding systems, the angular dependence is weak (Taylor and Kennard, 1982, 1984). For both complexes A and B the interaction energy varies by ~k_BT in a range of ~60° around the minimum energy geometry; there is a large angular region surrounding the N—H4 and C2—H5 groups in which a stable association with water is possible.

At the equilibrium r_{OH} distance (Fig. 5 *A*) of complex A, the interaction energy increases sharply at values of the N—H4· · ·O acceptor angle θ > 240° and θ < 140°. Decomposition of the molecular mechanics interaction energy shows that the sharp increases are due to repulsive van der Waals interaction between the water oxygen and H6 and H1 of NMP. At the H· · ·O distance of 2.5 Å (Fig. 5 *C*), the interaction energy curve is somewhat flatter than at the equilibrium distance. For complex B, the repulsive walls at θ < 150° and θ > 230° are due to interactions between the water oxygen and atom H7 and two methyl hydrogens of NMP (Fig. 5 *B*). The ab initio θ curves at r_{OH} = 2.5 Å exhibit shallow double minima with small barriers between them (Fig. 5 *D*). The minima and barriers are approximately reproduced by the molecular mechanics potential function.

To perform quantum chemical calculations on the retinal protonated Schiff base, we use the semiempirical method, AM1. To estimate the accuracy of AM1 in treating the aspects of retinal under investigation here, results for the model Schiff base (NMP) were compared with those obtained using the higher level, ab initio method. A qualitative accord was found for the geometries and energies of the molecules and complexes with some significant differences. The AM1 optimized geometry for the isolated NMP molecule is listed in Table 1. The geometries are in reasonable accord insofar as the bond lengths and angles are within ~0.03 Å and ~2–3° of the ab initio values. The intermolecular hydrogen-bonding distance in the AM1 optimized complex A is 2.04 Å, ~10% longer than the ab initio distance (1.87 Å). The donor angle N—H4· · ·O is ~23° narrower than the ab initio RHF/6–31G* result (175°). However, as was seen in the ab initio results, the AM1 angular potential is very flat over a range

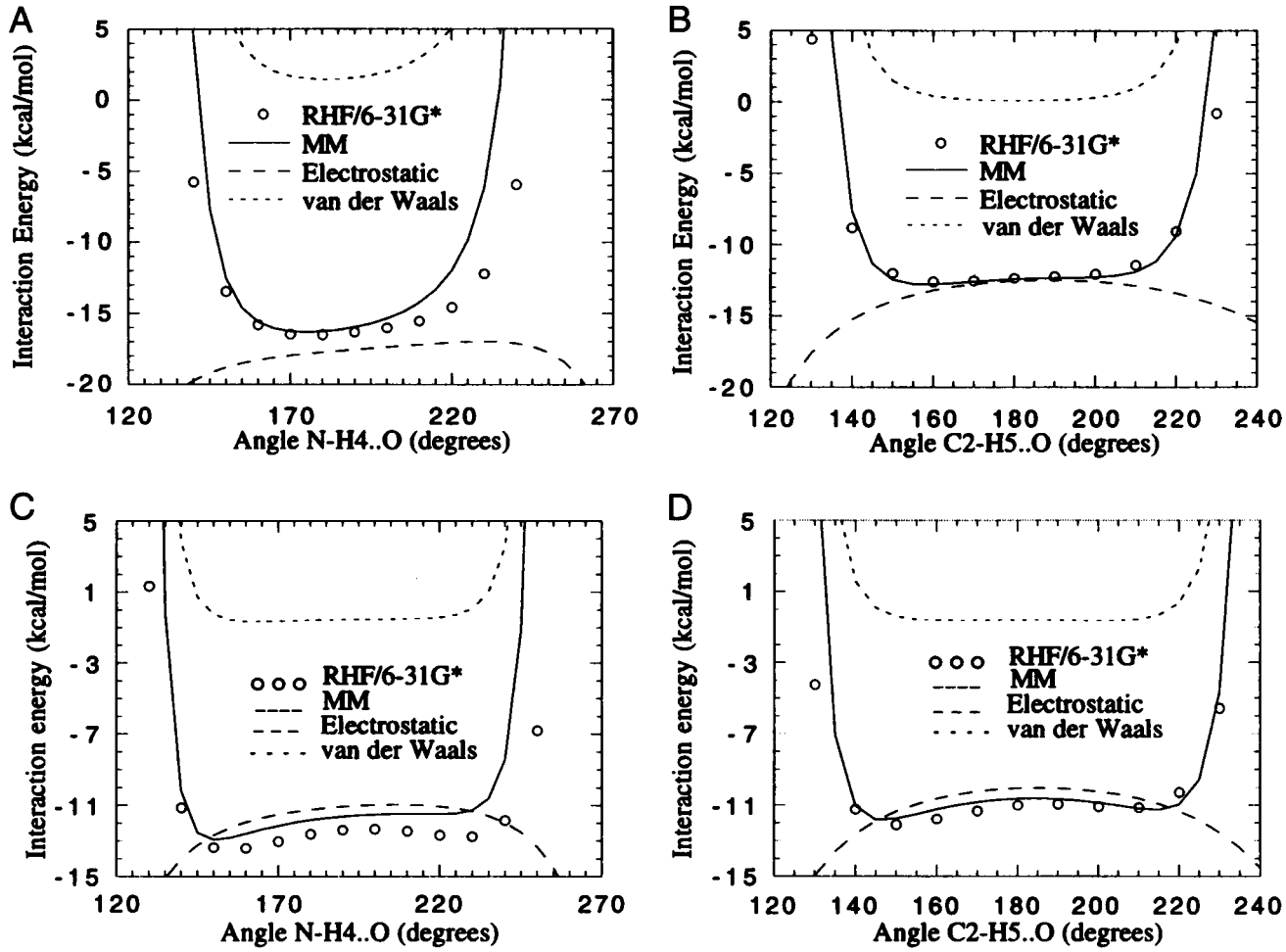

FIGURE 5 Angular dependence of the NMP-water complexes A and B interaction energies from ab initio and molecular mechanics calculations. Components of the molecular mechanical interaction energy are also plotted. (*A*) complex A with the hydrogen bond distance H4· · ·O fixed at the minimum energy distance 1.87 Å. (*B*) complex B with the hydrogen bond distance H5· · ·O fixed at the minimum energy distance 2.10 Å. (*C*) complex A with the hydrogen bond distance H4· · ·O fixed at 2.5 Å. (*D*) complex B with the hydrogen bond distance H5· · ·O for complex B is fixed at 2.5 Å.

of ~80°; the AM1 energy difference between the minimum-energy geometry (N—H4· · ·O = 152.5°) and the linear geometry is ~0.2 kcal/mol. Therefore, the difference in the minimum energy θ values is not considered to be significant. For complex B, the C2—H5· · ·O distance is 2.11 Å, very similar to that in RHF/6–31G* calculation (2.10 Å). The associated angle C2—H5· · ·O is found to be ~151°, ~18° narrower than the corresponding ab initio result (~169°). Again, the AM1 angular potential was found to be very flat.

The AM1 semiempirical interaction enthalpies for complexes A and B are −10.8 kcal/mol and −9.2 kcal/mol, respectively. These results are in qualitative agreement with the ab initio interaction energies in that they predict that the N—H4 and C2—H5 groups are both hydrogen-bonding and that the water: N—H4 interaction is stronger than that with C2—H5. No attempt was made to convert the ab initio interaction energies into interaction enthalpies for direct comparison with AM1. However, an estimation of this effect can be made by referring to previous work on similar hydrogen-bonding systems such as tetramethylammonium-water (Zheng and Merz, 1992; Koller and Hadzi, 1993). This would suggest that the interaction enthalpies are ~10% lower than the corresponding interaction energies. If this were the case, then the semiempirical method would give an interaction enthalpy ~4 kcal/mol lower than the ab initio method in complex A and ~2 kcal/mol lower in complex B. A further difference between AM1 and the ab initio is in the potential for rotation about C2—C3 bond. For this the AM1 value for the *trans-gauche* barrier is 4.3 kcal/mol compared with the ab initio value of 9.9 kcal/mol.

The NPR polyene chain-optimized AM1 geometry is listed in Table 3 together with the geometry derived from the experimental retinal structure (Hamanaka et al., 1972) and molecular mechanics optimized geometry. All C—C single bonds in the polyene chain are shorter in the AM1 calculations by ~0.01–0.03 Å, and all double bonds are longer by ~0.03–0.05 Å. The polyene chain bond angles are ~1°–2° narrower than in the x-ray structure with the exception of the C6—C7=C8 angle, which is ~7° wider. Geometry opti-

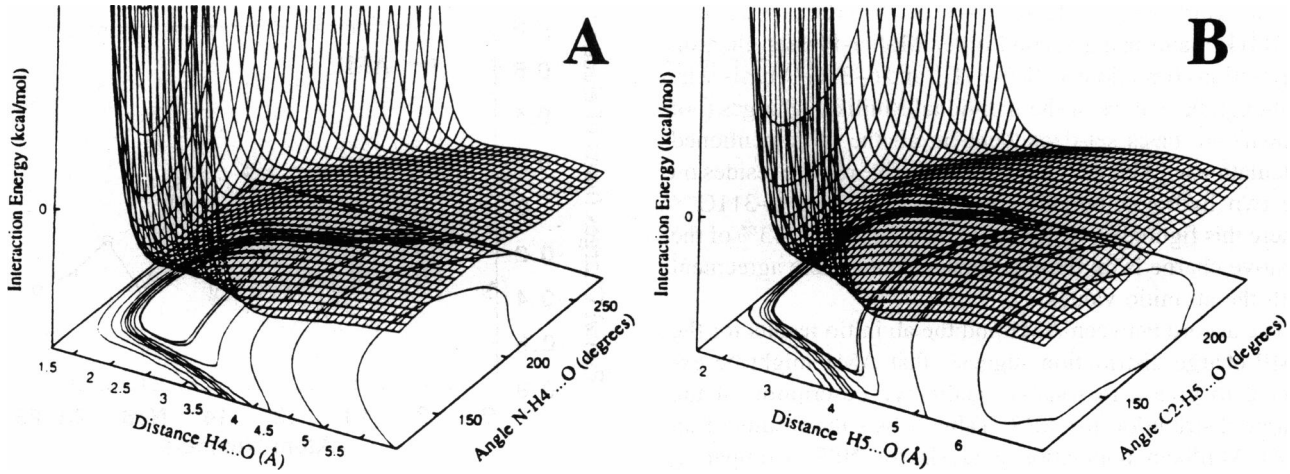

FIGURE 6 Molecular mechanical interaction energy surfaces (r_{OH}, θ). (*A*) complex A. (*B*) complex B.

TABLE 3 NPR polyene chain geometries derived from x-ray crystallography (Hamanaka et al., 1972), AM1, and molecular mechanical (MM) optimizations

	Exp.	AM1	MM
Bond lengths (Å)			
C6—C7	1.484	1.453	1.518
C7=C8	1.317	1.352	1.338
C8—C9	1.468	1.447	1.488
C19—C9	1.491	1.481	1.523
C9=C10	1.346	1.373	1.366
C10—C11	1.444	1.417	1.452
C11=C12	1.339	1.373	1.350
C12—C13	1.446	1.420	1.476
C13=C14	1.342	1.392	1.367
C20—C13	1.494	1.482	1.528
C14—C15	1.432	1.405	1.460
C15=N16	1.282	1.333	1.279
Bond angles (deg)			
C6—C7=C8	124.4	131.2	126.3
C7=C8—C9	126.5	124.7	128.8
C8—C9=C10	118.4	117.8	116.9
C9=C10—C11	127.2	126.0	129.2
C10—C11=C12	123.6	122.2	123.6
C11=C12—C13	126.0	124.7	128.3
C12—C13=C14	118.2	118.3	115.6
C13=C14—C15	125.9	125.2	128.3
C14—C15=N16	123.2	123.8	122.2

mization of *trans*-butadiene with AM1 results in the single bond being shorter by ~0.01 Å and the double bonds longer by ~0.01 Å than the corresponding RHF/6–31G* values. This suggests that C—C bond shortening and C=C bond lengthening compared with high level ab initio and experimental values may be systematic in AM1 calculations on these polyene molecules. The molecular mechanics and x-ray bond lengths agree to within 0.03 Å, and the bond angles agree to within 3°. The RMS coordinate deviation between the x ray and the molecular mechanics polyene chain is 0.30 Å.

The semiempirical method was used to investigate complexes between water molecules and the full retinal protonated Schiff base molecule, NPR. The interaction enthalpies calculated for the optimized complexes are −7.61 kcal/mol for complex A and −6.73 kcal/mol for complex B. These results suggest that increasing the polyene chain length decreases the interaction energy. In NPR-water complex A, the hydrogen-bonding distance is 2.08 Å, lengthening by ~0.04 Å from the NMP value. In NPR-water complex B, the intermolecular distance H15· · ·O is 2.12 Å, almost identical to that for NMP (2.11 Å).

Retinal charge distribution

AM1 and ab initio charge distributions for the isolated Schiff base, NMP, derived by Mulliken population analyses are listed in Table 4. Reasonable agreement between the ab initio and AM1 results is seen. The semiempirical charges are mostly smaller than the ab initio charges but agree in sign. The C15—H15 group is the most positive group, and the H16 atom binding the nitrogen is the most highly charged hydrogen. Ab initio calculations of the NMP Mulliken charge distribution were made using several different basis sets

TABLE 4 Net atomic charges for NMP derived from AM1 and ab initio RHF/6–31G* Mulliken Population Analysis (in units of electron charge)

Names	Ab initio	AM1	Names	Ab initio	AM1
C4 C13	−0.301	−0.123	N N16	−0.651	−0.305
H7 H13A	0.252	0.209	H4 H16	0.452	0.344
H8 H13B	0.276	0.243	C1 C16	−0.328	−0.268
C3 C14	−0.250	−0.355	H1 H16A	0.231	0.190
H6 H14	0.265	0.252	H1 H16B	0.252	0.211
C2 C15	0.254	0.123	H1 H16C	0.252	0.211
H5 H15	0.297	0.269			

at the Hartree-Fock level: 6–31G, 6–31G*, 6–31G**, 6–311G** and using second-order Møller-Plesset electron correlation corrections with 6–31G* and 6–31G** basis sets. Although the values of the individual Mulliken charges (not shown) are basis set-dependent, in all the aforementioned calculations ~35% of the total net positive charge resides on the two hydrogen-bonding groups (except for 6–311G** where this figure is ~40%). In the AM1 analysis, 43% of the positive charge is on these groups, in reasonable agreement with the ab initio values.

The accord between AM1 and the ab initio results for the NMP charge distribution suggests that AM1 might be expected to give a reasonable qualitative description of the charge distribution for NPR. Table 5 lists the results of an AM1 Mulliken population analysis for NPR. Comparing Tables 4 and 5 it is clear that in going from the small protonated Schiff base to the larger one, the N16 negative charge increases whereas the positive charge on the H16 binding the nitrogen atom and on H15 decrease. The C14 negative charge increases, and the H14 positive charge decreases by ~0.03 units of electron charge. The analysis results in a positive partial charge on odd carbons of the polyene chain whereas even carbons are negatively charged. A damped spatial oscillation of the charges is observed going from the C15 atom to C6 along the polyene chain, as shown in Fig. 7. Infrared absorption and ^{13}C NMR experiments on a compound $[CH_3(CH{=}CH)_5CH{=}NC_4H_9]^+$, which is closely related to the protonated Schiff base retinal, indicate that the positive charge is distributed on alternate odd carbon atoms on this molecule also (Blatz and Tompkins, 1993). Another effect present in the semiempirical calculations is the increase in bond alternation near the β-ionone ring of the chain, i.e., the double bonds become shorter and the single bonds become longer further away from the nitrogen atom. This effect has been seen in valence bond calculations on polyenes (Said et al., 1984) and in high resolution crystallographic studies of retinal (Santarsiero and James, 1990). Our geometry optimization of hexatriene at the MP2/6–31G** level confirms this effect, with the inner C=C bond lengths being 1.351 Å and the outer being 1.344 Å. The valence bond calculations (Said et al., 1984) indicate that the C=C bond length variations are accompanied by torsional barrier modifications, i.e., the shorter double bonds possess higher barriers. The C=C torsional barriers used in the present molecular mechanics force field are taken from the valence bond work.

The molecular mechanics atomic charge set for NPR is given in the Appendix. Partial charges for the

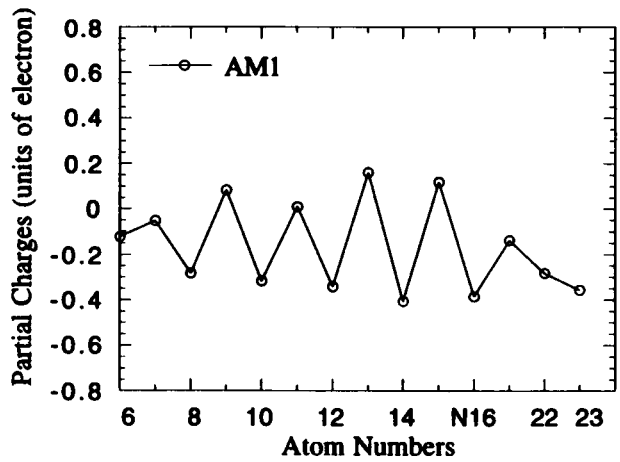

FIGURE 7 Charge distribution along the polyene chain carbon atoms of NPR from AM1 Mulliken population analysis.

[· · ·C14H14—C15H15=N16H16· · ·] moiety were directly transferred from the atomic charges, q_i, of NMP. The molecular mechanical partial charges possess a damped oscillation as seen in the AM1 calculation. The net positive charge (~23% of the total charge) on the NMP C13H13 group was distributed over the C13 atom and the methyl group binding the C13 atom. The charges for the propyl group binding the nitrogen atom were chosen as a compromise between those of the Lys side chain in the CHARMM 22 force field and the AM1 charge distribution.

The parameterization of the nonbonded terms of the force field was based mostly on ab initio calculations involving complexes of the retinal Schiff base with water molecules. Nevertheless, the energy function is expected also to represent reasonably well the nonbonded interactions of retinal with the other atoms in bR.

Molecular mechanics energy minimizations of bR

An important question is whether water molecules can be directly hydrogen-bonded to the protonated Schiff base in bR. To investigate further this possibility, we transferred the coordinates of the optimized complexes A and B as depicted in Fig. 2 to the bR experimental structure. In the directly transferred (non-energy-minimized) geometry, the complex A (NH) water molecule makes additional hydrogen bonds, with the Asp-212 and Asp-85 side chains. The oxygen atom of the complex B (CH) water molecule makes a small number of unfavorable contacts with the Leu-93 side chain.

TABLE 5 Net atomic charges for NPR derived from AM1 Mulliken Population Analysis

C6	−0.122	C10	−0.317	C13	0.162	CD	−0.283
C7	−0.052	H10	0.214	C14	−0.406	HD1	0.162
H7	0.175	C11	0.010	H14	0.226	HD2	0.135
C8	−0.284	H11	0.187	C15	0.120	CG	−0.357
H8	0.212	C12	−0.341	H15	0.239	HG1	0.159
C9	0.083	H12	0.220	N16	−0.386	HG2	0.137
C19	−0.364	C20	−0.384	H16	0.322	HG3	0.128
H19A	0.165	C20A	0.139	CE	−0.137		
H19B	0.164	C20B	0.177	HE1	0.144		
H19C	0.137	C20C	0.179	HE2	0.213		

Local relaxation of the hydrated structure was examined using two energy minimizations; one of bR with the complex A water molecule and one of bR with both the complex A and the complex B water molecules. The incorporated geometries were energy-minimized using the developed force field and the protocols described in Materials and Methods. In both minimizations no hydrogen bonds were formed directly between the retinal and the protein. The water molecules remained hydrogen-bonded to the Schiff base: the (N)H··O (H_2) distance is 1.70 Å in both minimizations, and the (C)H··O(H_2) distance is 2.03 Å in the minimization with two water molecules. The water molecules form additional hydrogen bonds with protein residues. The complex A water hydrogen-bonds to Asp-85 and Asp-212 in both minimizations. The Schiff base interacts with Asp-85 and Asp-212 via water-bridging, in accord with previous simulation work (Humphrey et al., 1994). The complex B water molecule hydrogen-bonds to the backbone carbonyl group of Ala-215. The small number of unfavorable contacts between the complex B water and Leu-93 were removed after minimization. The energy-minimized geometry with one water molecule is depicted in Fig. 8.

The interaction energy of the complex A water with the rest of the protein is ~ -40 kcal/mol in both minimizations. That of the complex B water is ~ -20 kcal/mol. The difference in the interaction energy of the two water molecules is ~20 kcal/mol. Because the difference in the Schiff base-water interaction energy is only ~4 kcal/mol (Table 2), the protein environment plays a major role in the preferential stabilization of the complex A water.

The interaction energies are much larger than the free energy of solvation of one water molecule in bulk solvent (Jorgensen et al., 1989). This provides a strong indication that the presence of water molecules is favorable near the retinal inside bR. Nevertheless, although the results are suggestive, they do not prove categorically that those sites must be occupied by water molecules under physiological conditions. To make a rigorous state-

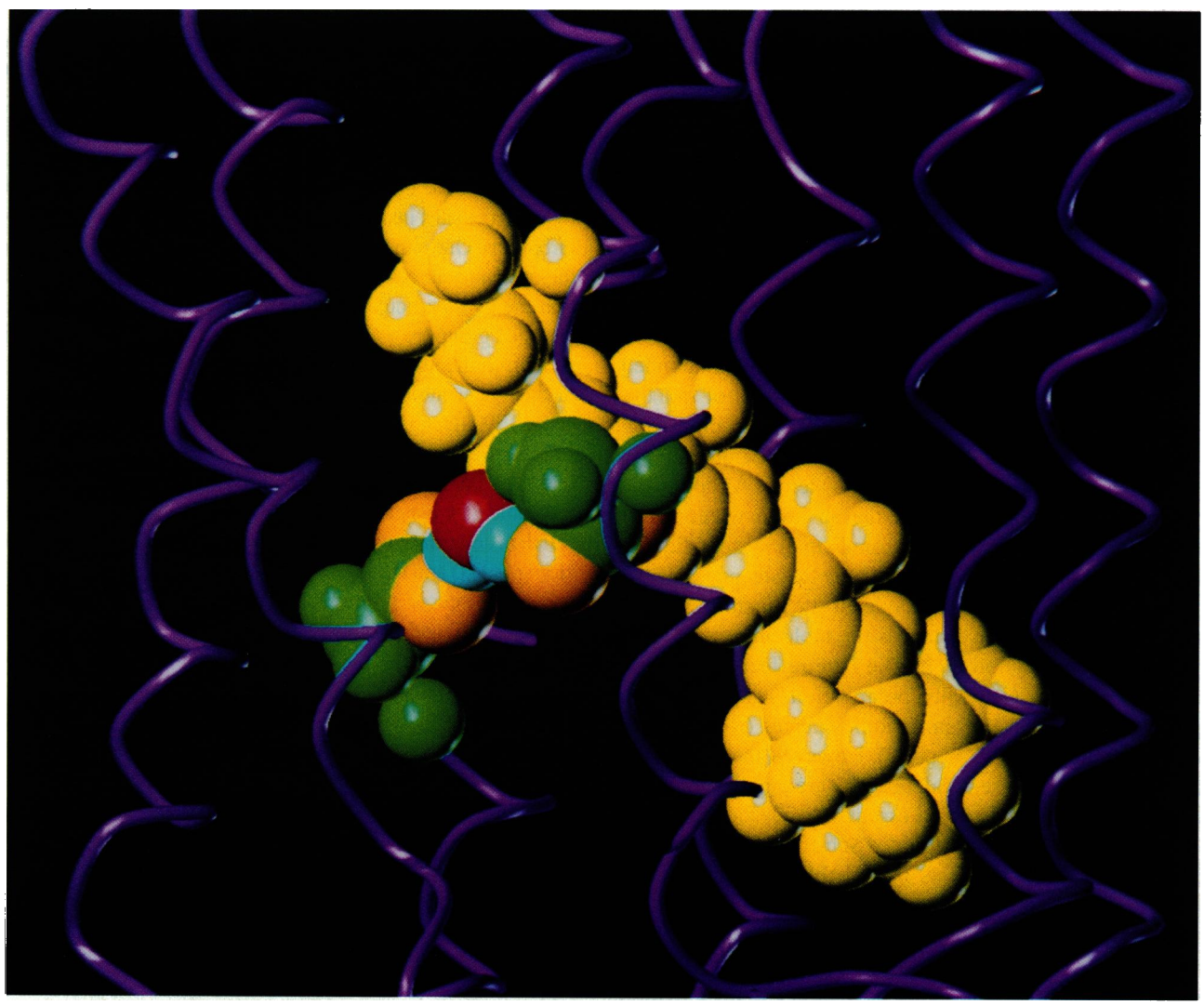

FIGURE 8 Model of retinal in bacteriorhodopsin with one water molecule bound to the NH group of the Schiff base, after energy-minimization of a 10 Å sphere with the molecular mechanical force field. The water molecule is in red and blue. The retinal is yellow. Also shown are the side chains of the Asp-212 (to the right of the water) and Asp-85 (in *green* with their carboxylate oxygens in *yellow*) and the bR helix backbone pathways.

ment about the thermodynamic stability of water at particular sites inside a protein, it is necessary to compare free energies. Appropriate computational approaches based on free energy simulations have been developed to calculate the binding constant of water molecules inside the cavities of proteins (Wade et al., 1991). Calculations are presently underway to investigate the binding free energies of waters inside bR.

CONCLUSION

In the work presented here, hydrogen-bonding and conformational energetics of the bacteriorhodopsin retinal protonated Schiff base were determined using a combination of computational methods. Two Schiff base-water hydrogen bonds are found to be possible, one on the cytoplasmic side of bR and one on the extracellular side. That the Schiff base NH group can form a hydrogen bond with water was expected. The hydrogen bond on the cytoplasmic side is of the relatively less well characterized C—H· · ·O type. C—H· · ·O hydrogen bonds can be particularly strong when they involve an N^+—C—H· · ·O interaction (Parker, 1994), as in the present case, because delocalization of the positive charge over the CH group increases its favorable electrostatic interaction with a water dipole. The quantum chemical calculations have allowed a quantification of the hydrogen bond interaction energies. For both complexes studied, the interaction energies are strong compared with the water dimer.

The results of the force field parameterization demonstrate that the molecular mechanics potential function is capable of accurately reproducing quantum mechanical values for the geometries, interaction energies, and conformational flexibility of the protonated Schiff base moiety. The nonbonded terms in the potential function consist of a sum of radially symmetric pair-decomposable site-site functions comprising Coulomb partial-charge electrostatics and Lennard-Jones 6–12 (core repulsion and van der Waals) terms. Although the energy function represents well the ab initio water-Schiff base interaction energy curves, some small systematic differences are present. At short distances the steepness of the core repulsion in the Lennard-Jones 6–12 function is overestimated, and at longer distances the molecular mechanics energies are slightly too high. The latter effect is probably due to polarization. Generally, polarization is expected to be significant in the case of small ionic species (Roux, 1993; Roux and Karplus, 1995, in press). However, the systematic differences in the present calculations are small, indicating that polarization terms are not essential to reproduce the interaction of water with a protonated Schiff base. The absence of strong polarization effects is probably due to the delocalization of the positive charge over the Schiff base cation and the relatively small polarizability of the water molecule (Jorgensen et al., 1993). Although a softer core repulsion and explicit polarization terms could be included in the potential function, the differences between the ab initio and molecular mechanics interaction energy curves in the low-energy range of interest are not sufficient to warrant changing the standard form of the CHARMM energy function in the present case.

The semiempirical results are of use in investigating qualitative trends in increasing conjugation of the polyene chain. However, significant differences between AM1 and the ab initio method were seen in the geometries and conformational energetics of the fragments examined. In particular, there is some evidence that the Schiff base-water interaction enthalpies are underestimated using AM1, in accord with previous calculations in cationic-neutral and nitrogen-based systems (Zheng and Merz, 1992). Nevertheless, the semiempirical work does suggest that the interaction energies decrease on increasing the conjugation length. Consequently, the pairwise interaction energies in the present model, derived from quantum chemical calculations on a system of short conjugation length, may be slightly overestimated. However, this overestimation may in itself compensate for many-body polarization effects that should also be present the protein. This is expected to be particularly noticeable for the NH (complex A) water, which makes additional hydrogen bonds with charged residues of the protein. It is likely that future ab initio quantum chemical studies will include the charge environment of the water-retinal complexes.

The interactions of water molecules with the Schiff base and retinal in the bR protein environment were investigated using the potential energy function. The molecular mechanics energy minimizations including the protein correspond to a relaxation of the structure into a minimum close to the starting geometry. The results indicate that water molecules can be incorporated in two distinct sites inside the protein without major structural perturbations. One site is near the NH group of the Schiff base, and the other is near a retinal CH group. The water-protein interaction energy is particularly strong for the water bound to the Schiff base NH group (~ -40 kcal/mol). The calculations thus provide support to the number of experiments that suggest the presence of this water molecule in bR (Harbison et al., 1988; De Groot et al., 1990; Deng et al., 1994) and is in general accord with the results of a molecular dynamics trajectory using a slightly different potential function (Humphrey et al., 1994). This water molecule may play an important role in the proton transfer in the canal, in determining the pK of adjacent residues (Sampogna and Honig, 1994) and retinal (Gat and Sheves, 1993), in determining the spectroscopic properties of retinal in bR (Grossjean and Tavan, 1988) and in conformational changes in the photocycle (Zhou et al., 1993). The results also indicate the existence of a site in a hydrophobic channel above the Schiff base where a water can hydrogen-bond with a retinal CH group (~ -20 kcal/mol interaction energy). A water molecule at such location might also play an important functional role, e.g., by facilitating the proton transfer between Asp-96 and the Schiff base (Cao et al., 1991). Further investigations based on the potential function developed here will be used to compute binding constants of water molecules at specific locations inside bR. Such calculations will prove useful in determining the likelihood of presence of water molecules adjacent to the Schiff base and in the "hydrophobic" channel of bR.

We thank Marc Gingold and Alain Sanson for computing assistance. Financial support is acknowledged from NATO and from the Commissariat à l'Energie Atomique. B. Roux is supported by a grant from the MRC of Canada.

APPENDIX

Parameters for molecular mechanics energy function

TABLE A Atom names, atom types, and partial charges (in units of electrons) for NMP and NPR

Name	Type	q_i	Name	Type	q_i	Name	Type	q_i	Name	Type	q_i	Name	Type	q_i
NMP														
C13	CR1	−0.103	C14	CR2	−0.180	H15	HPMA	0.189	C16	CTR	−0.001	H16C	HAR	0.147
H13A	HPLA	0.167	H14	HPLA	0.180	N16	NCHA	−0.727	H16A	HAR	0.147			
H13B	HPLA	0.167	C15	CR3	0.362	H16	HCRA	0.505	H16B	HAR	0.147			
NPR														
C1	CT	0.000	H16C	HA	0.090	C7	CR7	−0.100	H11	HPLB	0.090	N16	NCHB	−0.727
H18	CT	−0.270	C2	CT	−0.200	H7	HPLB	0.100	C12	CR12	−0.110	H16	HCRB	0.505
H18A	HA	0.090	H2A	HA	0.100	C8	CR8	−0.100	H12	HPLB	0.110	CE	CT	0.340
H18B	HA	0.090	H2B	HA	0.100	H8	HPLB	0.100	C20	CT	−0.170	HE1	HA	0.050
H18C	HA	0.090	C3	CT	−0.200	C9	CR9	0.000	C20A	HA	0.090	HE2	HA	0.050
C17	CT	−0.270	H3A	HA	0.100	C19	CT	−0.270	C20B	HA	0.090	CD	CT	−0.180
H17A	HA	0.090	H3B	HA	0.100	H19A	HA	0.090	C20C	HA	0.090	HD1	HA	0.090
H17B	HA	0.090	C4	CT	−0.200	H19B	HA	0.090	C13	CR13	0.131	HD2	HA	0.090
H17C	HA	0.090	H4A	HA	0.100	H19C	HA	0.090	C14	CR14	−0.180	CG	CT	0.180
C16	CT	−0.270	H4B	HA	0.100	C10	CR10	−0.100	H14	HPLB	0.180	HG1	HA	0.090
H16A	HA	0.090	C5	CR5	0.000	H10	HPLB	0.100	C15	CR15	0.362	HG2	HA	0.090
H16B	HA	0.090	C6	CR6	0.000	C11	CR11	−0.090	H15	HPMB	0.189	HG3	HA	

TABLE B Lennard-Jones parameters

Type	$r_{min}/2$ (Å)	$\epsilon_{i,i}$ (kcal/mol)	Type	$r_{min}/2$ (Å)	$\epsilon_{i,i}$ (kcal/mol)
NCH*	1.9500	−0.2000	HAR	1.4680	−0.0078
CTR	1.8000	−0.1562	HCR*	0.2245	−0.0460
CT	1.8000	−0.1562	HPM*	0.8700	−0.0078
CR*	2.1000	−0.1100	HPL*	0.8700	−0.0460
HA	1.4680	−0.0078			

TABLE C Bond length parameters

		k_b (kcal/mol/Å²)	b_0 (Å)			k_b (kcal/mol/Å²)	b_0 (Å)
CR1	CR2	600.0	1.329	CR9	CT	187.0	1.491
CR2	CR3	400.0	1.444	CR13	CT	187.0	1.493
CR5	CR6	250.0	1.329	CR5	CT	187.0	1.513
CR6	CR7	250.0	1.484	CTR	NCHA	515.0	1.470
CR7	CR8	250.0	1.317	CR*	NCH*	435.0	1.274
CR8	CR9	250.0	1.468	NCHB	CT	290.0	1.430
CR9	CR10	250.0	1.346	NCH*	HCR*	440.0	1.013
CR10	CR11	250.0	1.444	HPLA	CR*	330.0	1.075
CR11	CR12	250.0	1.339	HPMA	CR3	330.0	1.077
CR12	CR13	250.0	1.454	HAR	CTR	315.0	1.081
CR13	CR14	250.0	1.346	HPL*	CR1*	330.0	1.081
CR14	CR15	400.0	1.458	CT	HA	317.1	1.111
CR6	CT	187.0	1.534				

TABLE D Bond angles parameters

			k_θ (kcal/mol/rad²)	θ_0 (deg)				k_θ (kcal/mol/rad²)	θ_0 (deg)				k_θ (kcal/mol/rad²)	θ_0 (deg)
HPLB	CR7	CR6	41.0	117.8	CR7	CR8	CR9	95.0	126.5	CR12	CR13	CT	45.8	118.3
HPLB	CR7	CR8	41.0	117.8	CR8	CR9	CR10	95.0	118.4	CR14	CR13	CT	45.8	123.5
HPLB	CR8	CR7	41.0	116.8	CR9	CR10	CR11	95.0	127.2	CR6	CR5	CT	45.8	123.1
HPLB	CR8	CR9	41.0	116.8	CR10	CR11	CR12	95.0	123.6	CR5	CT	CT	51.8	115.2
HPLB	CR10	CR9	41.0	116.4	CR3	CR2	CR1	95.0	119.7	CR6	CT	CT	51.8	110.3
HPLB	CR10	CR11	41.0	116.4	HPLA	CR1	CR2	85.0	122.3	CT	CR5	CT	51.1	113.1
HPLB	CR11	CR10	41.0	118.2	HPLA	CR2	CR1	70.0	122.3	CR15	NCHB	HCRB	58.0	118.1
HPLB	CR11	CR12	41.0	118.2	HPMA	CR3	NCHA	50.0	117.3	CR15	NCHB	CT	50.0	124.7
HPLB	CR12	CR11	41.0	117.0	HAR	CTR	NCHA	95.0	109.8	HPMB	CR15	NCHB	50.0	117.3
HPLB	CR12	CR13	41.0	117.0	CR11	CR12	CR13	95.0	126.0	CR14	CR15	NCHB	70.0	123.8
HPLB	CR14	CR13	70.0	117.1	CR12	CR13	CR14	95.0	118.2	CT	NCH1	HCRB	35.0	117.2
HPMB	CR15	CR14	50.0	118.9	CR13	CR14	CR15	95.0	125.9	NCHB	CT	CT	70.0	113.5
HPLB	CR14	CR15	50.0	118.1	CR7	CR6	CR5	60.0	122.6	NCHB	CT	HA	51.5	109.5
HA	CT	CR5	49.3	107.5	CR5	CR6	CT	45.8	122.4	NCHA	CR3	CR2	70.0	123.8
HA	CT	CR9	49.3	107.5	CR7	CR6	CT	45.8	115.0	CTR	NCHA	HCRA	35.0	117.2
HA	CT	CR13	49.3	107.5	CR8	CR9	CT	45.8	118.4	HAR	CTR	NCHA	95.0	108.3
CR6	CR7	CR8	95.0	124.4	CR10	CR9	CT	45.8	123.3	HAR	CTR	NCHA	95.0	109.8

TABLE E Torsional parameters

				k_ϕ (kcal/mol)	n	δ (deg)					k_ϕ (kcal/mol)	n	δ (deg)
CR*	CR*	CR*	CR*	0.1600	1	0.0	CT	CT	NCHB	CR15	0.300	1	0.0
CR*	CR*	CR*	CR*	2.2318	2	180.0	CT	CT	NCHB	HCRB	0.300	1	0.0
CR*	CR*	CR*	CR*	1.1324	3	0.0	X	CR7	CR8	X	5.625	2	180.0
CR*	CR*	CR*	CR*	0.3006	4	0.0	X	CR9	CR10	X	4.625	2	180.0
CR*	CR*	CR*	NCH*	1.504	1	180.0	X	CR11	CR12	X	4.375	2	180.0
CR*	CR*	CR*	NCH*	5.301	2	180.0	X	CR1	CR2	X	8.000	2	180.0
CR*	CR*	CR*	NCH*	0.916	3	0.0	X	NCH*	CR*	X	8.000	2	180.0
CR*	CR*	CR*	NCH*	0.401	4	0.0							

Definition of torsional parameters: X refers to wild card specification. Torsions are independent of 1,4 interactions. The intrinsic torsional energy is evaluated separately for each torsion angles X-A-B-Y. The contribution of a given torsional parameter to the intrinsic barrier is evaluated by multiplying the torsional force constant by twice the number of 1,4 interactions.

REFERENCES

Blatz, P. E., and J. A. Tompkins. 1993. Relative ground and excited state energies of $CH_3(CH{=}CH)_5\ CH{=}NC_4H_9$, its hydrogen-bonded and proton-transferred species, and charge partitioning and distribution in the protonated Schiff base of retinal. *Photochem. Photobiol.* 58: 400–408.

Bousché, O., M. S. Braiman, Y. W. Ye, T. Marti, H. G. Khorana, and K. J. Rothschild. 1991. Vibrational spectroscopy of bacteriorhodopsin mutants. *J. Biol. Chem.* 266:11063–11067.

Braiman, M. S., T. Mogi, T. Marti, L. J. Stern, H. G. Khorana, and K. J. Rothschild. 1988. Vibrational spectroscopy of bacteriorhodopsin mutants: light-driven proton transport involves protonation changes of aspartic acid residues 85, 96, and 212. *Biochemistry.* 27:8516–8520.

Braiman, M. S., O. Bousché, and K. J. Rothschild. 1991. Protein dynamics in the bacteriorhodopsin photocycle: submillisecond Fourier transform infrared spectra of the L, M, and N photointermediates. *Proc. Natl. Acad. Sci. USA.* 88:2388–2392.

Brooks, B. R., R. E. Bruccoleri, B. D. Olafson, D. J. States, S. Swaminathan, and M. Karplus. 1983. CHARMM: a program for macromolecular energy minimization and dynamics calculations. *J. Comp. Chem.* 4:187–217.

Burkert, U., and N. L. Allinger. 1982. Molecular Mechanics. American Chemical Society, Washington D.C.

Butt, H. J., K. Fendler, E. Bamberg, J. Tittor, and D. Oesterhelt. 1989. Aspartic acids 96 and 85 play a central role in the function of bacteriorhodopsin as a proton pump. *EMBO J.* 8:1657–1663.

Cao, Y., G. Váró, M. Chang, B. Ni, R. Needleman, and J. K. Lanyi. 1991. Water is required for proton transfer from Asp 96 to the bacteriorhodopsin Schiff base. *Biochemistry.* 30:10972–10979.

De Groot, H. J. M., S. O. Smith, J. Courtin, E. van der Berg, C. Winkel, J. Lugtenburg, R. G. Griffin, and J. Herzfeld. 1990. Solid-state ^{13}C and ^{15}N NMR study of the low pH forms of bacteriorhodopsin. *Biochemistry.* 29:6873–6882.

Deng, H., L. Huang, R. Callender, and T. Ebrey. 1994. Evidence for a bound water molecule next to the retinal Schiff base in bacteriorhodopsin and rhodopsin: a resonance Raman study of the Schiff base hydrogen/deuterium exchange. *Biophys. J.* 66:1129–1136.

Deng, H., L. Huang, M. Groesbeek, J. Lugtenburg, and R. H. Callender. 1994. Vibrational analysis of a retinal protonated Schiff base analog. *J. Phys. Chem.* 98:4776–4779.

Dewar, M. J. S., E. G. Zoebisch, E. F. Healy, and J. J. P. Stewart. 1985. AM1: a new general purpose quantum mechanical molecular model. *J. Am. Chem. Soc.* 107:3902–3909.

Frisch, M. J., J. E. Del Bene, J. S. Binkley, and H. F. Schaefer III. 1986. Extensive theoretical studies of the hydrogen-bonded complexes $(H_2O)_2$, $(H_2O)_2H^+$, $(HF)_2$, $(HF)_2H^+$, F_2H^-, and $(NH_3)_2$. *J. Chem. Phys.* 84:2279–2289.

Frisch, M. J., M. Head-Gordon, G. W. Trucks, J. B. Foresman, H. B. Schlegel, K. Raghava-chari, M. Robb, J. S. Binkley, C. Gonzalez, D. J. Defrees, D. J. Fox, R. A. Whitesick, R. Seeger, C. F. Melius, J. Baker, R. L. Martin, L. R. Kahn, J. J. P. Stewart, S. Topiol, and J. A. Pople. 1990. GAUSSIAN 90. Carnegie-Mellon University, Pittsburgh, PA.

Gat, Y., and M. Sheves. 1993. A mechanism for controlling the pK_a of the retinal protonated Schiff base in retinal proteins. A study with model compounds. *J. Am. Chem. Soc.* 115:3772–3773.

Gerwert, K., G. Souvignier, and B. Hess. 1990. Simultaneous monitoring of light-induced changes in protein side-group protonation, chromophore isomerization, and backbone motion of bacteriorhodopsin by time-resolved Fourier-transform infrared spectroscopy. *Proc. Natl. Acad. Sci. USA.* 87:9774–9778.

Grossjean, M. F., and P. Tavan. 1988. Wavelength regulation in bacteriorhodopsin and halorhodopsin: a Pariser-Parr-Pople multireference double excitation configuration interaction study of retinal dyes. *J. Chem. Phys.* 88:4884–4896.

Guo, H., and M. Karplus. 1991. Ab initio studies of polyenes. I. 1,3-butadiene. *J. Chem. Phys.* 94:3679–3699.

Hamanaka, T., T. Mitsui, T. Ashida, and M. Kakudo. 1972. The crystal structure of all-*trans* retinal. *Acta Cryst.* B28:214–222.

Harbison, G. S., S. O. Smith, J. A. Pardoen, C. Winkel, J. Lugtenburg, J. Herzfeld, R. A. Mathies, and R. G. Griffin. 1984a. Dark-adapted bacteriorhodopsin contains 13-cis, 15-syn and all-trans, 15-anti retinal Schiff base. *Proc. Natl. Acad. Sci. USA.* 81:1706–1709.

Harbison, G. S., S. O. Smith, J. A. Pardoen, P. P. J. Mulder, J. Lugtenburg, J. Herzfeld, R. A. Mathies, and R. G. Griffin. 1984b. Solid-state ^{13}C-NMR studies of retinal in bacteriorhodopsin. *Biochemistry.* 23: 2662–2667.

Harbison, G. S., J. E. Roberts, J. Herzfeld, and R. G. Griffin. 1988. Solid-state NMR detection of proton exchange between the bacteriorhodopsin Schiff base and bulk water. *J. Am. Chem. Soc.* 110:7221–7227.

Hehre, W. J., L. Radom, P. V. R. Schleyer, and J. A. Pople. 1986. *Ab initio* Molecular Orbital Theory. Wiley Interscience, New York.

Henderson, R., J. M. Baldwin, T. A. Ceska. F. Zemlin, E. Beckmann, and K. H. Downing. 1990. Model for the structure of bacteriorhodopsin based on high-resolution electron cryomicroscopy. *J. Mol. Biol.* 213:899–929.

Hildebrandt, P., and M. Stockburger. 1984. Role of water in bacteriorhodopsin's chromophore; resonance Raman study. *Biochemistry.* 23:5539–5548.

Holz, M., L. A. Drachev, T. Mogi, H. Otto, A. D. Kaulen, M. P. Heyn, V. P. Skulachev, and H. G. Khorana. 1989. Replacement of aspartic acid-96 by asparagine in bacteriorhodopsin slows both the decay of the M intermediate and the associated proton movement. *Proc. Natl. Acad. Sci. USA.* 86:2167–2171.

Humphrey, W., I. Logunov, K. Schulten, and M. Sheves. 1994. Molecular dynamics study of bacteriorhodopsin and artificial pigments. *Biochemistry.* 33:3668–3678.

Jorgensen, W. L., J. Chandrasekhar, J. D. Madura, R. W. Impey, and M. L. Klein. 1983. Comparison of simple potential functions for simulating liquid water. *J. Chem. Phys.* 79:926–935.

Jorgensen, W. L., J. F. Blake, and J. F. Bucker. 1989. Free energy of TIP4P water and the free energies of CH_4 and Cl^- from statistical perturbation theory. *Chem. Phys.* 129:193–200.

Jorgensen, W. L., and D. L. Severance. 1993. Limited effects of polarization for $Cl^-(H_2O)_n$ and $Na^+(H_2O)_n$ clusters. *J. Chem. Phys.* 99:4233–4235.

Koller, J., and D. Hadzi. 1993. Ab initio and semiempirical calculations on the interaction of tetramethylammonium with a water molecule. *J. Mol. Struct.* 279:311–319.

Kontoyianni, M., A. J. Hoffman, and J. P. Bowen. 1992. Ab initio and molecular mechanical calculations on imine derivatives: a study of the rotational barriers and the development of MM2 parameters. *J. Comp. Chem.* 13:57–65.

Lifson, S., A. T. Hagler, and P. Dauber. 1979. Consistent force field studies of intermolecular forces in hydrogen-bonded crystals. 1. Carboxylic acids, amides, and the C=O· · ·H hydrogen bonds. *J. Am. Chem. Soc.* 101:5111–5141.

Marti, T., H. Otto, T. Mogi, S. J. Rösselet, M. P. Heyn, and H. G. Khorana. 1991. Bacteriorhodopsin mutants containing single substitutions of serine or threonine residues are all active in proton translocation. *J. Biol. Chem.* 266:6919–6927.

Mathies, R. A., S. W. Lin, J. B. Ames, and W. T. Pollard. 1991. From femtoseconds to biology: mechanism of bacteriorhodopsin's light-driven proton pump. *Annu. Rev. Biophys. Biophys. Chem.* 20:491–518.

Mogi, T., L. J. Stern, N. R. Hackett, and H. G. Khorana. 1987. Bacteriorhodopsin mutants containing single tyrosine to phenylalanine substitutions are all active in proton translocation. *Proc. Natl. Acad. Sci. USA.* 85:5595–5599.

Mogi, T., L. J. Stern, T. Marti, B. H. Chao, and H. G. Khorana. 1988. Aspartic acid substitutions affect proton translocation by bacteriorhodopsin. *Proc. Natl. Acad. Sci. USA.* 84:5595–5599.

Mulliken, R. S. 1955. Electronic population analysis on LCAO-MO molecular wave functions. I. *J. Chem. Phys.* 23:1833–1840.

Nina, M., B. Roux, and J. C. Smith. 1992. Ground state potential surface calculations for butadiene and retinal. *In* Structures and Functions of Retinal Proteins. J. L. Rigaud, editor. Colloque INSERM/John Libbey Eurotext Ltd. 221:17–20.

Nina, M., J. C. Smith, and B. Roux. 1993. Ab initio quantum chemical analysis of water-Schiff base interactions in bacteriorhodopsin. *J. Mol. Struct.* (THEOCHEM) 286:231–245.

Oesterhelt, D., and W. Stoeckenius. 1971. Rhodopsin-like protein from the purple membrane of *Halobacterium halobium. Nature.* 233: 149–152.

Oesterhelt, D., and W. Stoeckenius. 1973. Functions of a new photoreceptor membrane. *Proc. Natl. Acad. Sci. USA.* 70:2853–2857.

Otto, H., T. Marti, M. Holz, T. Mogi, M. Lindau, H. G. Khorana, and M. P. Heyn. 1989. Aspartic acid-96 is the internal proton donor in the reprotonation of the Schiff base of bacteriorhodopsin. *Proc. Natl. Acad. Sci. USA.* 86:9228–9232.

Papadopoulos, G., N. Dencher, G. Zaccaï, and G. Büldt. 1990. Water molecules and exchangeable hydrogen ions at the active centre of bacteriorhodopsin localized by neutron diffraction. *J. Mol. Biol.* 214: 15–19.

Parker, D. 1994. Solvation and complexation: from cation complexation to excited-state stabilisation. *In* Computational Approaches in Supramolecular Chemistry. G. Wipff, editor. NATO ASI Series. 221–235.

Pettei, M. J., A. P. Yudd, K. Nakanishi, R. Henselman, and W. Stoeckenius. 1977. Identification of retinal isomers isolated from bacteriorhodopsin. *Biochemistry.* 16:1955–1959.

Pfefferlé, J. M., A. Maeda, J. Sasaki, and T. Yoshizawa. 1991. Fourier transform infrared study of the N intermediate of bacteriorhodopsin. *Biochemistry.* 30:6548–6556.

Rath, P., T. Marti, S. Sonar, H. G. Khorana, and K. J. Rothschild. 1993. Hydrogen bonding interactions with the Schiff base of bacteriorhodopsin. Resonance Raman spectroscopy of the mutants D85N and D85A. *J. Biol. Chem.* 268:17742–17749.

Rothschild, K. J., P. V. Argade, T. N. Earnest, K.-S. Huang, E. London, M.-J. Liao, H. Bayley, H. G. Khorana, and J. Herzfeld. 1982. The site of attachment of retinal in bacteriorhodopsin. *J. Biol. Chem.* 257:8592–8595.

Rothschild, K. J., Y.-W. He, S. Sonar, T. Marti, and H. G. Khorana. 1992. Vibrational spectroscopy of bacteriorhodopsin mutants. Evidence that Thr-46 and Thr-89 form part of a transient network of hydrogen bonds. *J. Biol. Chem.* 267:1615–1622.

Roux, B. 1993. Nonadditivity in cation-peptide interactions: a molecular dynamics and ab initio study of Na^+ in the gramicidin channel. *Chem. Phys. Lett.* 212:231–240.

Said, M., D. Maynau, J.-P. Malrieu, and M.-A. Garcia Bach. 1984. A nonempirical Heisenberg hamiltonian for the study of conjugated hydrocarbons. Ground-state conformational studies. *J. Am. Chem. Soc.* 106:571–579.

Sampogna, R. V., and B. Honig. 1994. Environmental effects on the protonation states of active site residues in bacteriorhodopsin. *Biophys. J.* 66:1341–1352.

Santarsiero, B. D., and M. N. G. James. 1990. Crystal structure of N-methyl-N-phenylretinal iminium perchlorate: a structural model for the bacteriorhodopsin chromophore. *J. Am. Chem. Soc.* 112:9416–9418.

Smith, J. C., and M. Karplus. 1992. Empirical force field study of geometries and conformational transitions of some organic molecules. *J. Am. Chem. Soc.* 114:801–812.

Smith, S. O., J. Courtin, E. van den Berg, C. Winkel, J. Lugtenburg, J. Herzfeld, and R. G. Griffin. 1989. Solid state ^{13}C NMR of the retinal chromophore in photointermediates of bacteriorhodopsin: characterization of two forms of M. *Biochemistry.* 28:237–243.

Sperling, W., P. Carl, Ch. N. Rafferty, and N. A. Dencher. 1977. Photochemistry and dark equilibrium of retinal isomers and bacteriorhodopsin isomers. *Biophys. Struct. Mech.* 3:79–94.

Stern, L. J., and H. G. Khorana. 1989. Structure-function studies on bacteriorhodopsin. Individual substitutions of Arg residues by Gln affect chromophore formation, photocycle and proton translocation. *J. Biol. Chem.* 264:14202–14208.

Taylor, R., and O. Kennard. 1982. Crystallographic evidence for the existence of C—H· · ·O, C—H· · ·N, and C—H· · ·Cl hydrogen bonds. *J. Am. Chem. Soc.* 104:5063–5070.

Taylor, R., and O. Kennard. 1984. Hydrogen-bond geometry in organic crystals. *Acc. Chem. Res.* 17:320–326.

Ulrich, A. S., A. Watts, I. Wallat, and M. P. Heyn. 1994. Distorted structure of the retinal chromophore in bacteriorhodopsin resolved by ^2H-NMR. *Biochemistry.* 33:5370–5375.

Wade, R., M. H. Mazor, J. A. McCammon, and F. A. Quiocho. 1991. A molecular dynamics study of thermodynamic and structural aspects of the hydration of cavities in proteins. *Biopolymers.* 31:919–931.

Zheng, Y.-J., and K. M. Merz, Jr. 1992. Study of hydrogen bonding interactions relevant to biomolecular structure and function. *J. Comp. Chem.* 13:1151–1169.

Zhou, F., A. Windemuth, and K. Schulten. 1993. Molecular dynamics study of the proton pump cycle of bacteriorhodopsin. *Biochemistry.* 32: 2291–2306.

Zundel, G. 1986. Proton polarizability of hydrogen bonds: infrared methods, relevance to electrochemical and biological systems. *Methods Enzymol.* 127:439–455.